CHAPTER IV
RESULTS AND DISCUSSION

4.1 Carbon Aerogels Characterization

4.1.1 Surface and Pore Characteristics

A surface area and pore volume of carbon aerogels (CAs) depend on the concentration of benzoxazine precursor, which uses dimethylformamide (DMF) as a diluent via ambient pressure drying process, as shown in Table. 4.1. All investigated benzoxazine concentrations give a high surface area, which are 313, 341, and 312 m^2/g for 25, 35, and 45 % w/w of benzoxazine concentration, respectively. The different benzoxazine concentrations do not affect the surface areas. The micropore volume is in the range of 0.137 to 0.151 cm^3/g. However, there is a change in the mesopore volume, when 35 % w/w of benzoxazine was used to synthesize CAs. In this work, 25 % w/w of benzoxazine concentration was selected to study as this concentration shows good interconnected structures of CAs and requires the least time for the gelation process.

Table 4.2 summarizes the surface area of CAs prepared with different dioxane. The surface area of the sample with the DMF to dioxane mole ratio of 100 is 313 m^2/g, which is close to the surface areas of samples prepared with other mole ratios. However, the change in the ratio resulted in different micropore volumes. That is the lower the ratio, the lower the micropore volume. The opposite is true for the mesopore volume.

Table 4.1 Physical properties of synthesized carbon aerogels by varying benzoxazine concentration

Concentration	Surface area (m^2/g)	Micropore volume (cm^3/g)	Mesopore volume (cm^3/g)	Gelation time (hr)
25 % w/w	313	0.151	0.056	1.15
35 % w/w	341	0.137	0.172	1.3
45 % w/w	312	0.141	0.050	3

Table 4.2 Physical properties of carbon aerogels by varying dioxane solution

Mole ratios of DMF/Dioxane	Surface area (m^2/g)	Micropore volume (cm^3/g)	Mesopore volume (cm^3/g)
100/0	313.0	0.151	0.056
90/10	332.3	0.161	0.143
75/25	331.2	0.143	0.231
50/50	311.0	0.125	0.255

4.1.2 Microstructure Analysis

Microstructure of the CAs was investigated by using scanning electron micrograph as shown in Figure 4.1. The micrographs show that the synthesized CAs at the benzoxazine concentration of 25 and 35 % w/w (Figure 4.1A and 4.1B) show interconnected structure of cluster and consists of three-dimensional networks of carbon particles, while the benzoxazine concentration of 45 % w/w (Figure 4.1C) leads to aggregated carbon particles. The result implies that increasing the benzoxazine concentration induces the agglomeration of carbon particles.

The micrographs of CAs prepared from different DMF to dioxane mole ratios are shown in Figure 4.2. At a high mole ratio of DMF (Figure 4.2A), the structure of CAs consists of three-dimensional networks of carbon particles and fine surfaces that contain the different pore size. However, the lower ratio leads to carbon particle agglomeration and smooth surface that consists of large pore size. From the surface and pore characteristics, 25 % w/w of benzoxazine mixed with the 50/50 DMF to dioxane mole ratio was selected to further study because of its high surface area and mesopore volume, which may improve the desorption temperature and the desorption behaviors of $LiAlH_4$.

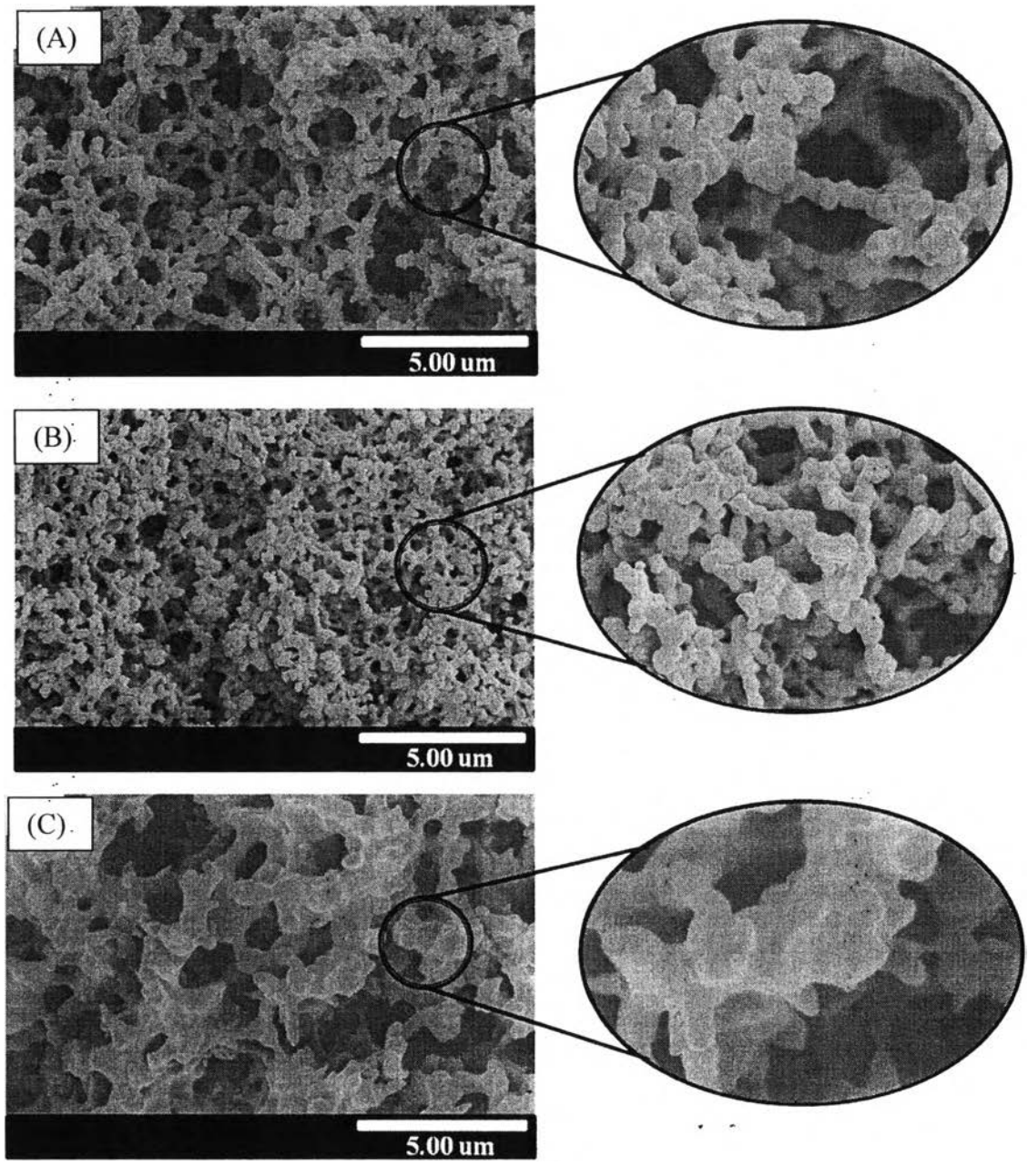

Figure 4.1 Scanning electron micrographs of synthesized CAs by varying benzoxazine concentration, 25%w/w (A), 35%w/w (B), 45%w/w (C).

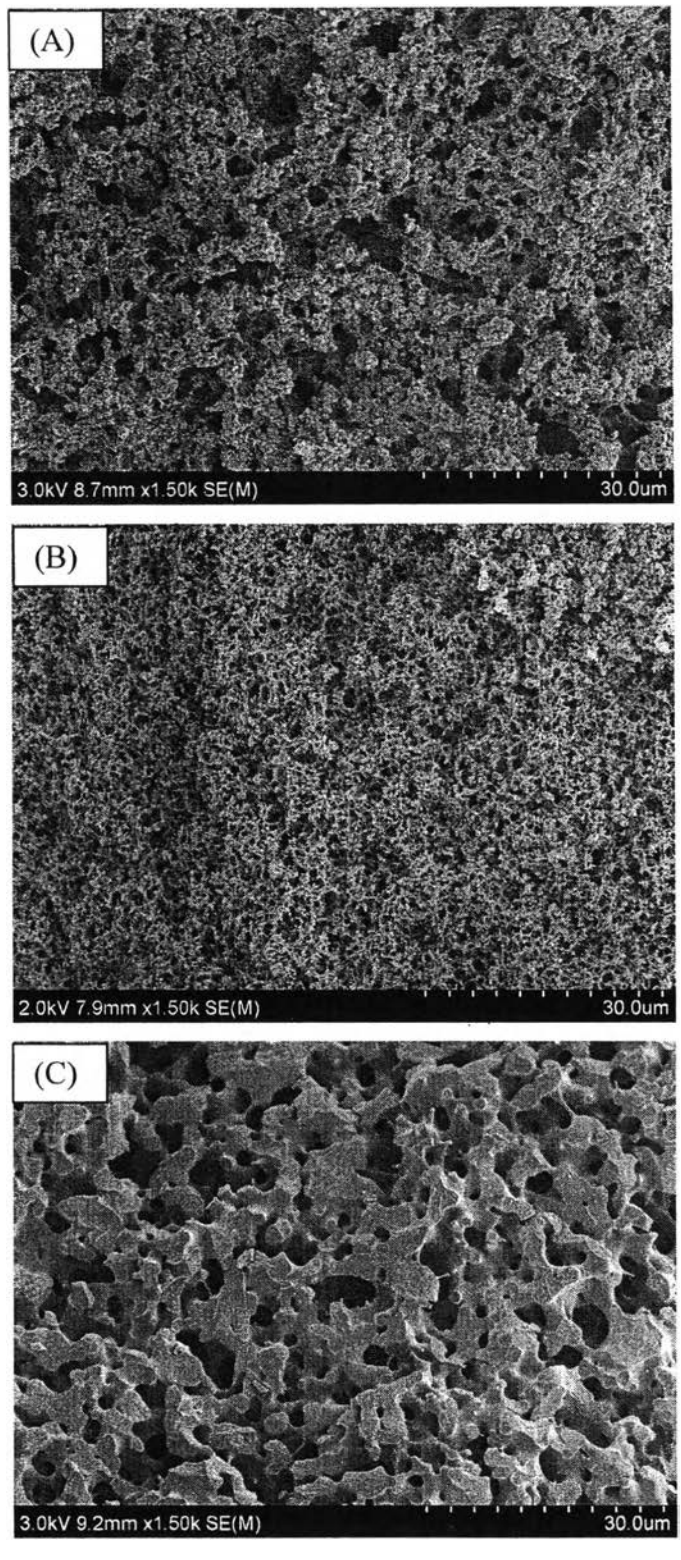

Figure 4.2 Scanning electron micrographs of polybenzoxzazine-based aerogel by mixing solvent of DMF and dioxane at ratio of 90/10 (A), 75/25 (B) and 50/50 (C).

4.2 Hydrogen Desorption Characterization

4.2.1 TPD Results

TPD curves were used to investigate the thermal desorption behaviors of mixed and unmixed $LiAlH_4$. Table 4.3 summarizes the desorption temperature of all tested samples from TPD curves. As-received $LiAlH_4$ releases hydrogen at 145 and 215 °C. Surprisingly, $LiAlH_4$ milled for 0.5 hr has the same hydrogen desorption behavior as the as-received sample in the first hydrogen desorption temperature, while the second hydrogen desorption temperature decreases by 10 °C for the milled sample compared with the as-received one.

The addition of CAs affects the hydrogen desorption behavior of $LiAlH_4$. It can be seen that mixing 5 wt% CAs with $LiAlH_4$ has very little effect on the first step of the desorption temperature as it has the same behavior as the as-received $LiAlH_4$ and $LiAlH_4$ milled 0.5 hr but its desorption temperature decreases to 195 °C. However, when 15 wt% CAs was used, the desorption temperature decreases by 30 and 20 °C. The result implies that mixing with a certain amount of CAs is needed to show any positive effects on the desorption temperature of $LiAlH_4$. The results are in agreement with Suttisawat *et al.* (2010), who concluded that the Al-H bond could be destabilized by adding an electronegative carbon substrate. In addition, Berseth *et al.* (2009) suggested that adding carbon nanotubes and C_{60} fullerences with $NaAlH_4$ alters the Al-H bonding; consequently, the Al-H bonding was weaken and the desorption temperature of $NaAlH_4$ was decreased to a lower temperature.

It is well known that catalysts are an important factor that affects the desorption temperature of $LiAlH_4$. This work further substantiates the effects of a catalyst on the desorption of $LiAlH_4$. It can be seen that mixing 5 wt% TiO_2, Degussa P 25, with $LiAlH_4$ has significant effects on the desorption temperature as mixing with $TiCl_3$. Samples mixed with TiO_2 and $TiCl_3$ have lower desorption temperatures, 95 and 175 °C. The results agree with Langmi *et al.* (2010) who concluded that $LiAlH_4$ doped with a low amount of $TiCl_3$ decreased the desorption temperature by 60 to 75 °C in the first desorption step. Mao *et al.* (2009) also reported that adding 5 mol% TiO_2 with $LiAlH_4$-$LiBH_4$ decreased the desorption temperatures in the first

and second desorption steps by 27 and 50 °C, respectively. However, at the same weight ratio, mixing with a catalyst has more pronounced affects on the desorption temperature than mixing with CAs.

Co-mixing between CAs and catalysts with $LiAlH_4$ was also studied. $LiAlH_4$ co-mixed with 5 wt% CAs and 5 wt% TiO_2 or $TiCl_3$ affects on the desorption temperature more than mixing with only 10 wt% CAs. For example, the desorption temperatures of the co-mixed sample with 5 wt% CAs and 5 wt% TiO_2 or $TiCl_3$ decreases to 95 and 170 °C in the first and second steps. Comparison between the co-mixed samples with the sample mixed with either a catalyst or CAs, shows that the addition of 5 wt% CAs does not affect the first desorption temperature, but it does on the second desorption temperature. In other words, while the catalysts contribute to the decrease in both first and the second desorption temperatures, CAs only affect the second one. The observation is similar to a report by Suttisawat *et al.* (2008), who concluded that the addition of graphite and TiO_2 affected both first and second temperatures of $NaAlH_4$.

Table 4.3 Desorption temperatures of $LiAlH_4$ mixed with CAs and catalysts

Sample	**Desorption temperature (°C)**	
	1st	**2nd**
As-received $LiAlH_4$	145	215
Milled $LiAlH_4$	145	200
Milled 5 wt% CAs-$LiAlH_4$	145	195
Milled 10 wt% CAs-$LiAlH_4$	130	185
Milled 15 wt% CAs-$LiAlH_4$	115	195
Milled 5 wt% Ti-$LiAlH_4$	110	195
Milled 5 wt% TiO_2-$LiAlH_4$	95	175
Milled 5 wt% $TiCl_3$-$LiAlH_4$	95	175
Milled 5 wt% Ni-$LiAlH_4$	105	195
Milled 5 wt% CAs/Ti-$LiAlH_4$	110	195
Milled 5 wt% CAs/TiO_2-$LiAlH_4$	95	170
Milled 5 wt% CAs/$TiCl_3$-$LiAlH_4$	95	170
Milled 5 wt% CAs/Ni-$LiAlH_4$	105	195

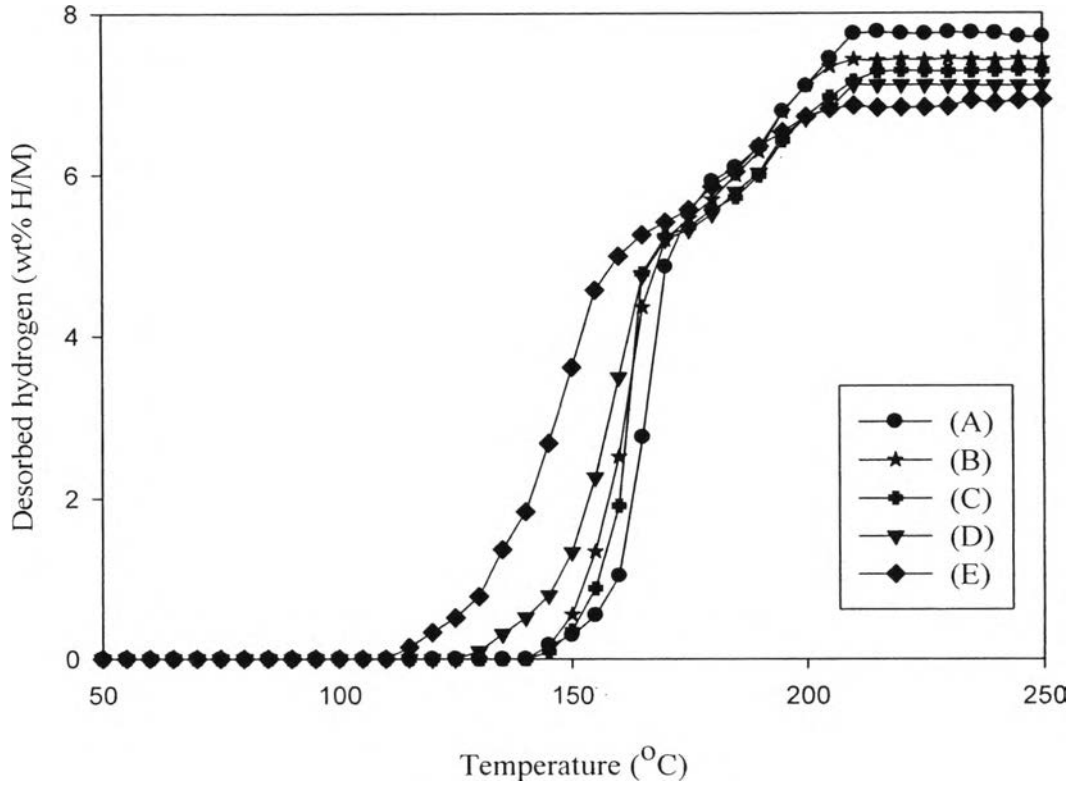

Figure 4.3 Hydrogen desorption from as-received $LiAlH_4$ (A), $LiAlH_4$ milled for 0.5 hr (B), and $LiAlH_4$ mixed with 5 wt% CAs (C), 10 wt% CAs (D), and 15 wt% CAs (E).

4.2.2 Thermo-volumetric Results

Figure 4.3 shows the effects of mixing CAs with $LiAlH_4$ compared to the as-received and ball milled samples. For the as-received sample, as shown in Figure 4.3A, it releases hydrogen in two steps. The first step occurs at 145 °C and releases about 5.3 wt% hydrogen. The second step releases 2.4 wt% hydrogen and takes place at 180 °C, with a total amount of desorbed hydrogen close to the theoretical hydrogen value, 7.9 wt% hydrogen. In addition, $LiAlH_4$ milled for 0.5 hr (Figure 4.3B) releases hydrogen only 7.5 wt% at the same condition and its desorption behavior is lower than the as-received sample. A reason for the loss may be from the hydrogen desorption during the ball milling step. Moreover, the samples mixed with CAs show different desorption temperatures and desorption behaviors. In

addition, the amounts of desorbed hydrogen from mixing with CAs are lower than that from the as-received sample because the partial decomposition during the preparation step, which is in agreement with Kumar *et al.* (2008). However, the addition of 5 wt% CAs has very little effect on the initial desorption temperature of $LiAlH_4$ (Figure 4.3C) compared to the as-received and milled samples (Figure 4.3A and 4.3B), while its desorbed hydrogen is 7.3 wt%, which is about the same as that of $LiAlH_4$ milled for 0.5 h. $LiAlH_4$ mixed with 15 wt% CAs (Figure 4.3E) exhibits the lowest desorption temperature. Its desorption temperature is reduced by 30 °C, and the amount of desorbed hydrogen is 6.9 wt%. That may be attributed to the high enough amount of CAs in $LiAlH_4$. Similar results were reported by Hudson *et al.* (2008), who reported that an increase in the mass ratios of helical graphite nanofiber in $LiMg(AlH_4)_3$ and $LiAlH_4$ led to the decrease in the hydrogen capacity. The desorption behavior of sample mixed with 5 wt% CAs show better than as-received and milled samples because the addition of CAs may increased the surface area of LiAlH4. As mixing 15 wt% CAs do not good desorption behavior due to adding high amount of CAs also increased the surface area, but it may suppress the hydrogen diffusion from bulk materials. Therefore, 5 wt% CAs was chosen to investigate effects of co-mixing with catalysts on the hydrogen desorption behavior of $LiAlH_4$.

The effect of adding catalysts is shown in Figure 4.4. Mixing any of the catalysts with $LiAlH_4$ reduces the desorption temperature significantly. Especially, $LiAlH_4$ mixed with 5 wt% TiO_2 or $TiCl_3$ (Figure 4.4C and 4.4D) has the lowest desorption temperature, 50 °C, and the amounts of desorbed hydrogen are about 7.3 wt%, which are lower than the as-received and milled $LiAlH_4$ samples. That may be because the reaction between $LiAlH_4$ and the Ti compounds, TiO_2 and $TiCl_3$, could form Al_3Ti, which acts as a catalyst that improves the desorption temperature (Liu *et al.*, 2009). In contrast, the desorption behaviors of adding either TiO_2 or $TiCl_3$ decreases slightly compared to as-received $LiAlH_4$. Kojima *et al.* (2008) suggested that the mechanochemical reaction between $LiAlH_4$ and metal chloride like $TiCl_3$, $ZrCl_4$, VCl_3, and $NiCl_2$ would generate the transition metal trialuminides, Al_3X (Ti, Zr, V, Ni). Therefore, reactions between $LiAlH_4$ and the Ti compounds may possibly occur following Equations (4.1) – (4.2),

$$3LiAlH_4 + TiCl_3 \rightarrow Al_3Ti + 3LiCl + 6H_2 \quad (4.1)$$

$$LiAlH_4 + Li_3AlH_6 + Al + TiO_2 \rightarrow Al_3Ti + 2Li_2O + 5H_2 \quad (4.2)$$

The addition of either Ti or Ni does affect the desorption temperature of $LiAlH_4$ but not to the extent contributed by TiO_2 or $TiCl_3$ (Figure 4.4C and 4.4F). It is worth noting that about the same desorbed hydrogen amount can be obtained from mixing with one of the four catalysts. Ti and Ni react with $LiAlH_4$ following Equations (4.3)-(4.4),

$$3LiAlH_4 + Ti \rightarrow Al_3Ti + 3LiH + 9/2H_2 \quad (4.3)$$

$$3LiAlH_4 + Ni \rightarrow Al_3Ni + 3LiH + 9/2H_2 \quad (4.4)$$

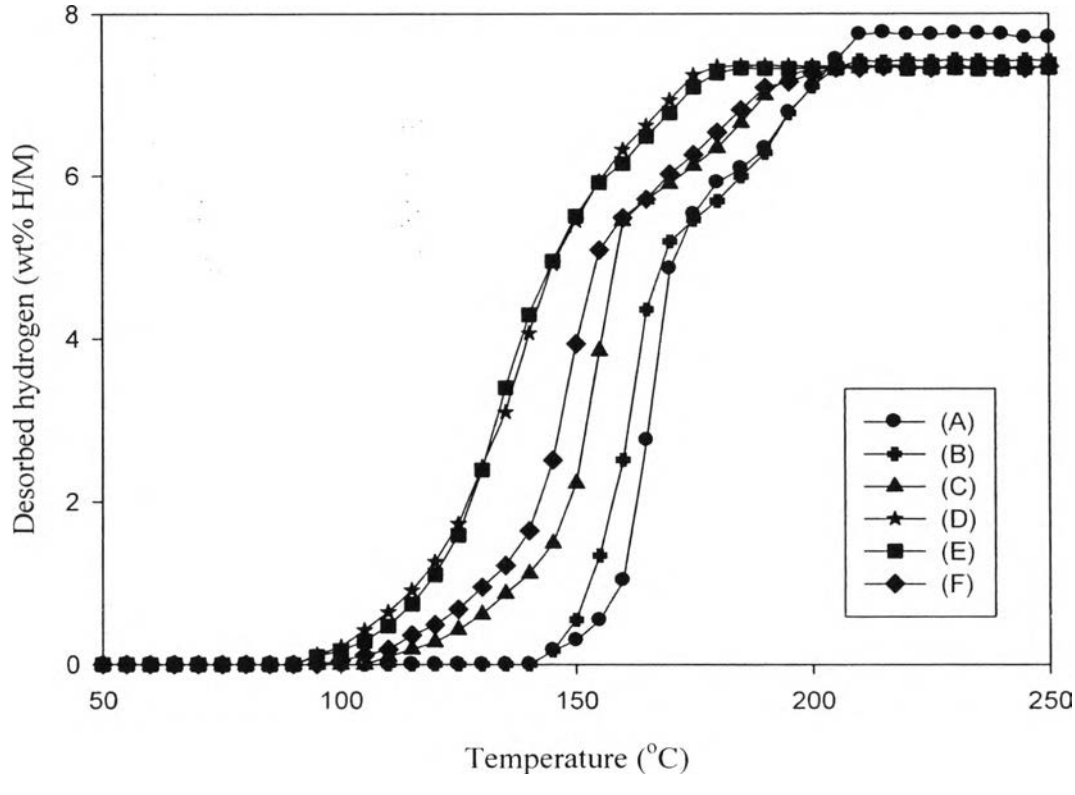

Figure 4.4 Hydrogen desorption from as-received $LiAlH_4$ (A), $LiAlH_4$ milled for 0.5 hr (B), and $LiAlH_4$ mixed with 5 wt% Ti (C), 5 wt% TiO_2 (D), 5 wt% $TiCl_3$ (E), and 5 wt% Ni (F).

From the results, it can be summarized that mixing a catalyst with $LiAlH_4$ resulted in a lower desorption temperature than mixing with CAs at the same weight ratio. $LiAlH_4$ mixed with 5 wt% TiO_2 or $TiCl_3$ decreases the first and second desorption temperature to 95 and 175 °C, while mixing 5 wt% CAs (Figure 4.3C) has no effect on the first desorption temperature, but it only affects the second desorption temperature, which is reduced by 20 °C. On the other hand, the desorption behaviors of the sample mixed with 5 wt% CAs is better than adding with either one of the catalysts.

$LiAlH_4$ mixed with CAs and catalysts was also investigated. The desorption temperature of the co-mixed samples occurs at the same temperature as mixing with the catalysts and the amounts of desorbed hydrogen of the co-mixed samples release 7.2 wt% hydrogen, which is close to the desorbed hydrogen for $LiAlH_4$ mixed with 5 wt% CAs and catalysts. $LiAlH_4$ mixed with 5 wt% CAs and TiO_2 or $TiCl_3$ (Figure 4.5C and 4.5D) shows the lowest desorption temperature, 90 and 170 °C. Their desorption behaviors are better than the samples mixed with the catalysts. That may be from the addition of 5 wt% CAs, which improves the desorption behaviors of $LiAlH_4$ samples. The results suggested that the co-mixed samples have lower the desorption temperatures than mixing CAs with $LiAlH_4$. In contrast, the desorption behaviors of the samples co-mixed with CAs and catalysts are slower than the samples mixed with CAs. It is believed that the catalysts have more influence on the desorption temperature than CAs, while CAs affect the desorption behaviors, which agrees with Zhu *et al.* (2010) results. They found that the addition of both catalysts and CAs showed better dehydrogenation behavior of MgH_2 than that of adding with either catalysts or CAs.

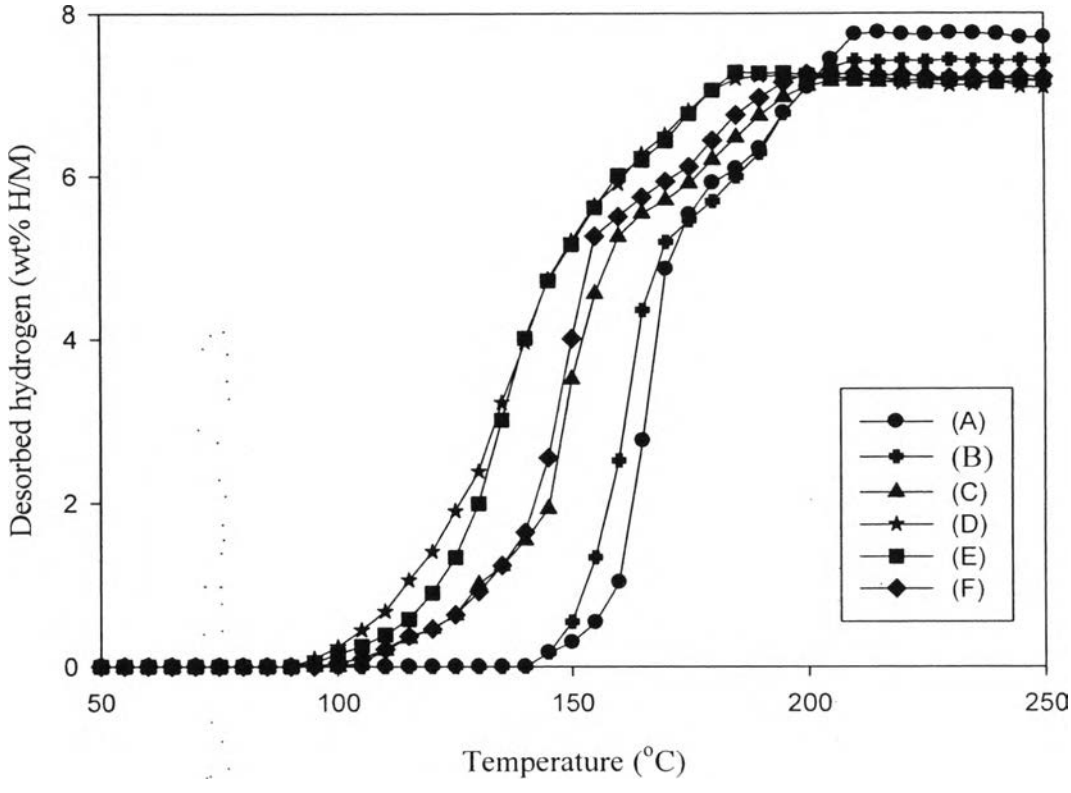

Figure 4.5 Hydrogen desorption from as-received $LiAlH_4$ (A), $LiAlH_4$ milled for 0.5 hr (B), and $LiAlH_4$ co-mixed with 5 wt% CAs and Ti (C), 5 wt% TiO_2 (D), 5 wt% $TiCl_3$ (E), and 5 wt% Ni (F).

4.2.3 XRD Results

The XRD results were used to analyze the phase of $LiAlH_4$. Blanchard *et al.* (2004) reported that $LiAlH_4$ releases hydrogen in the first step at 157 to 175 °C to form Li_3AlH_6, Al, and H_2 as shown in Equation (4.5). After that, the decomposition of Li_3AlH_6 into LiH, Al, and H_2 occurs at 180 to 220 °C, according to Equation (4.6). The last step releases hydrogen at a high temperature, 400 °C, which can be expressed by Equation (4.7).

$$3LiAlH4 \rightarrow Li_3AlH_6 + 2Al + 3H_2 \qquad (4.5)$$

$$Li_3AlH_6 \rightarrow 3LiH + Al + 3/2H_2 \qquad (4.6)$$

$$3LiH + 3Al \rightarrow 3LiAl + 3/2H_2 \qquad (4.7)$$

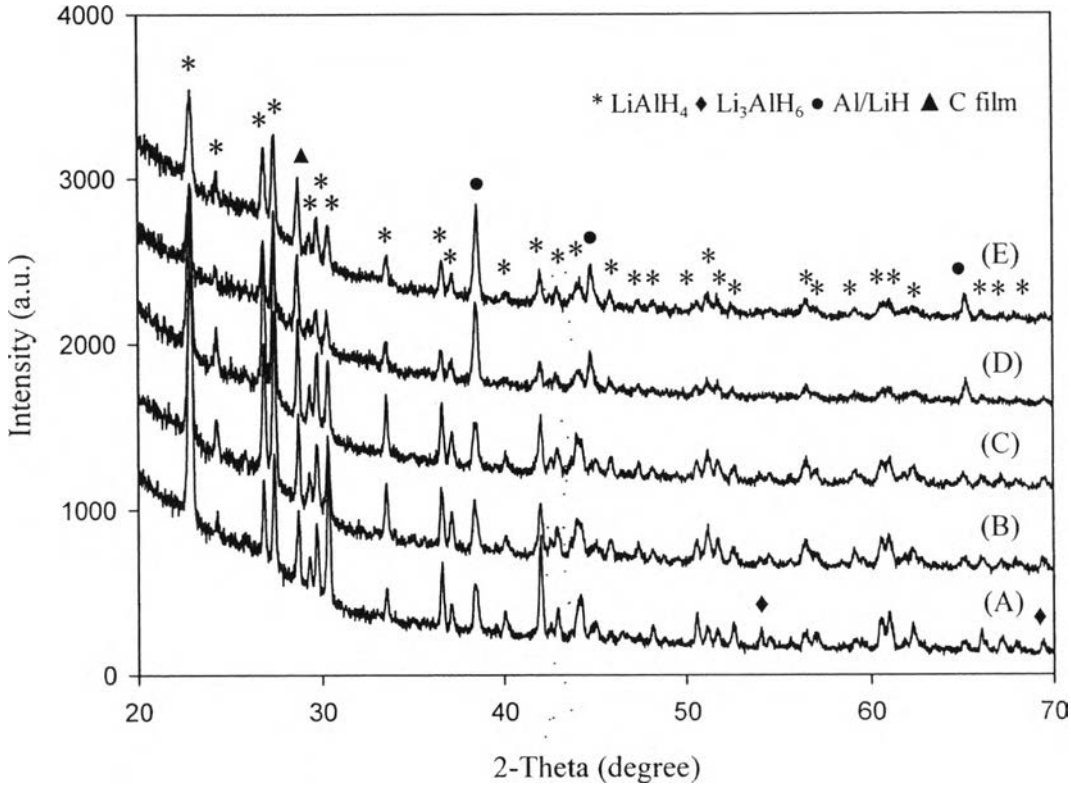

Figure 4.6 XRD patterns of as-received $LiAlH_4$ (A), $LiAlH_4$ milled for 0.5 hr (B), and $LiAlH_4$ mixed with 5 wt% CAs (C), 10 wt% CAs(D), and 15 wt% CAs (E).

Figure 4.6 shows XRD patterns of $LiAlH_4$ mixed with different weight ratios of CAs compared with the as-received and milled $LiAlH_4$ samples. The XRD pattern of the as-received sample (Figure 4.6A) consists of $LiAlH_4$, Li_3AlH_6, Al, LiH, and LiCl. The $LiAlH_4$ peaks for the as-received sample have higher intensity than the milled sample and the sample mixed with different weight ratios of CAs. In contrast, the intensity of Li_3AlH_6 and Al peaks of the milled sample (Figure 4.6B) is increased compared with the as-received sample, which is believed to be contributed from the partial decomposition of $LiAlH_4$ and Li_3AlH_6 to Li_3AlH_6, Al, LiH, and H_2 during the ball milling. Therefore, Equations (4.5) and (4.6) occur in the ball milling because of the energy accumulation. Mixing 5 wt% CAs with $LiAlH_4$ resulted in the same peaks like the milled sample, while the sample mixed with 15

wt% CAs exhibits higher intensity of Al peaks. The results also suggested that the amount of mixing CAs in the sample affects the phase change and hydrogen released during the ball milling because CAs have more unlocalized electron, which may be shared with $LiAlH_4$ and interact with hydrogen. That, in turn, affects the hydrogen desorption temperature (Wang *et al.*, 2010).

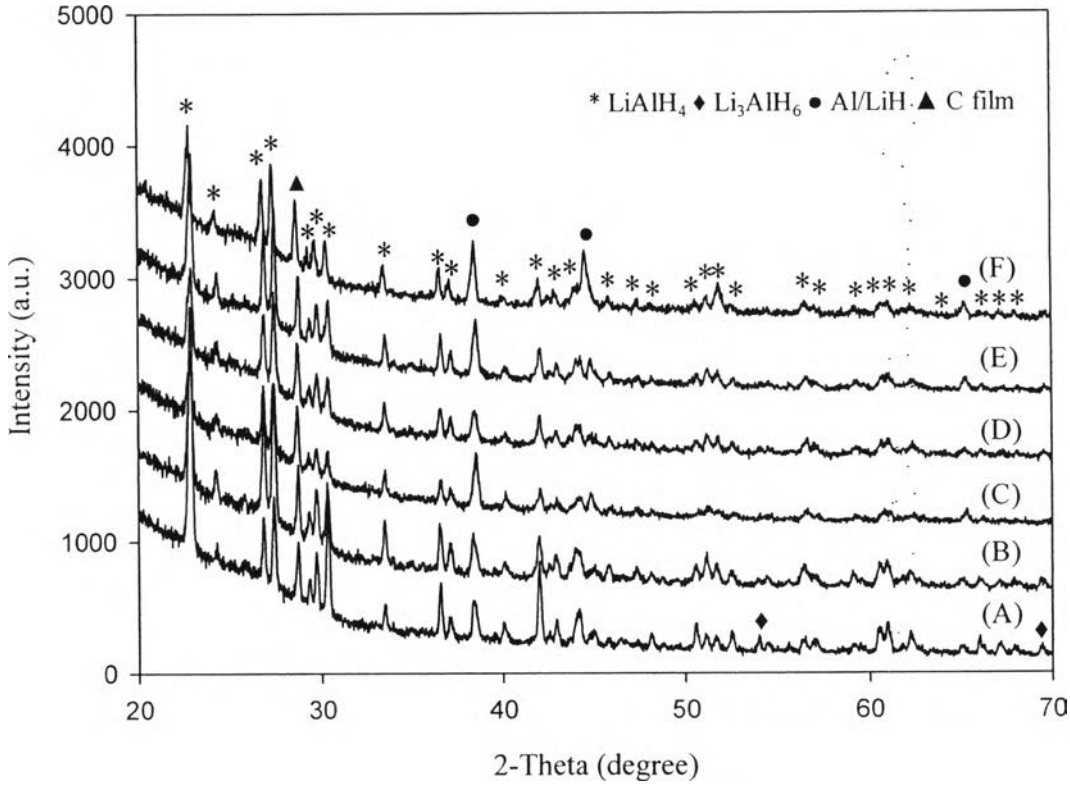

Figure 4.7 XRD patterns of as-received $LiAlH_4$ (A), $LiAlH_4$ milled for 0.5 hr (B), and $LiAlH_4$ mixed with 5 wt% Ti (C), 5 wt% TiO_2 (D), 5 wt% $TiCl_3$ (E), and 5 wt% Ni (F).

Catalysts are one factor that affects the phase of $LiAlH_4$ as shown in Figure 4.7. The XRD patterns of $LiAlH_4$ mixed with all catalysts, Ti, TiO_2, $TiCl_3$, and Ni, change slightly compared with the milled sample. In the presence of a catalyst, $LiAlH_4$ is transformed to Li_3AlH_6, Al, and H_2 by a mechanochemical reaction (Kojima *et al.*, 2008). In addition, $Al_{1-x}Ti_{1-x}$ compounds as an active species (Card No. 42-1137) to decrease the desorption temperature do not appear in the XRD pattern because they overlap with the Al peaks. The $Al_{1-x}Ti_{1-x}$ like Al_3Ti according to Equations (4.1)-(4.2) was reported by Liu *et al* (2009). In the case of the sample mixed with Ni, Al_3Ni, which also decreases the desorption temperature, may be formed following Equation (4.4). So the XRD results imply that all tested catalysts have little effect on the phase composition compared with CAs.

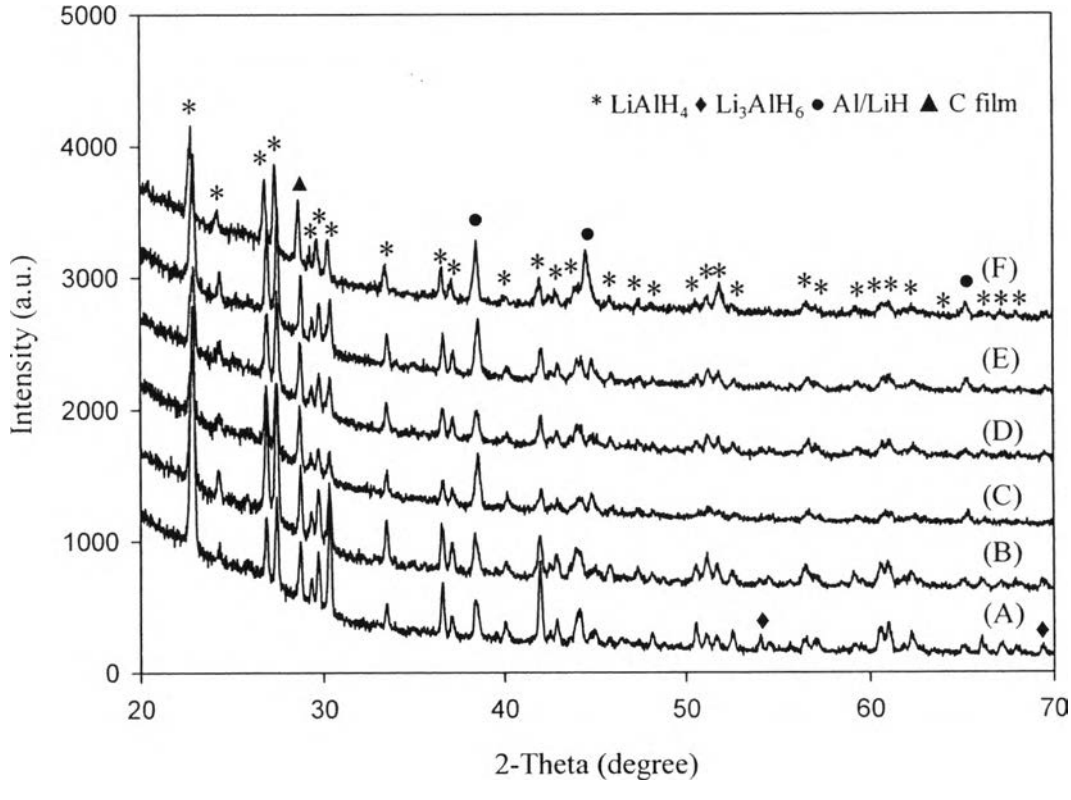

Figure 4.8 XRD patterns of as-received $LiAlH_4$ (A), $LiAlH_4$ milled for 0.5 hr (B), and $LiAlH_4$ co-mixed with 5 wt% CAs and 5 wt% Ti (C), 5 wt% TiO_2 (D), 5 wt% $TiCl_3$ (E), and 5 wt% Ni (F).

The XRD patterns of $LiAlH_4$ co-mixed with 5 wt% catalysts and 5 wt% CAs (Figure 4.8) are similar to those mixed with 5 wt% catalysts (Figure 4.7) or 5 wt% CAs (Figure 4.6). Again, it can be concluded that the phases of $LiAlH_4$ is influenced by the amounts of CAs, while mixing with the catalysts does not.

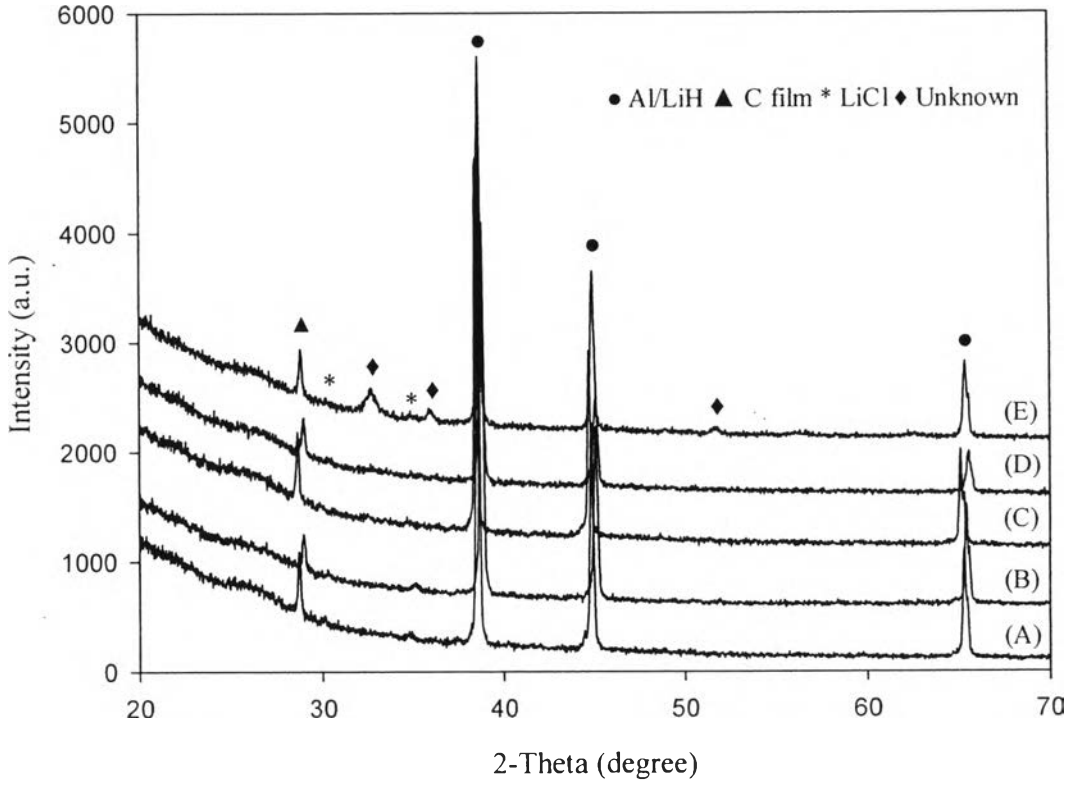

Figure 4.9 XRD patterns of dehydrogenated $LiAlH_4$ (A), dehydrogenated $LiAlH_4$ milled for 0.5 hr (B), and dehydrogenated $LiAlH_4$ mixed with 5 wt% CAs (C), 10 wt% CAs (D), and 15 wt% CAs (E).

The XRD patterns of the dehydrogenated samples mixed with different weight ratios of CAs, as-received $LiAlH_4$, and $LiAlH_4$ milled 0.5 h, are shown in Figure 4.9. LiH and Al are the products after the decomposition at 250 °C. For as-received $LiAlH_4$ (Figure 4.9A), Al peaks are sharper than the milled sample and that mixed with CAs because the unmilled sample changes its structure and morphology, sinters, and agglomerates solid, while either catalyzed or milled sample

maintain those properties after heating (Beattie and McGrady, 2009). The hydrogenated sample with 15 wt% CAs (Figure 4.8E), exhibits different peaks from that with 5 wt% (Figure 4.9C) and 10 wt% CAs (Figure 4.9D). Figure 4.8E shows a new phase, which cannot be identified. It is believed that they are not Li_2C_2 as its peaks are present at 2θ of 29 and 48.5° (Zhang *et al.*, 2007). The unknown peaks may be generated in the Li-Al-H-C systems, which shall be further studied. The result indicates that mixing with CAs would prevent the agglomeration of a complex metal hydride and preserves the grain size of the hydrogenated sample (Suttisawat *et al.*, 2010).

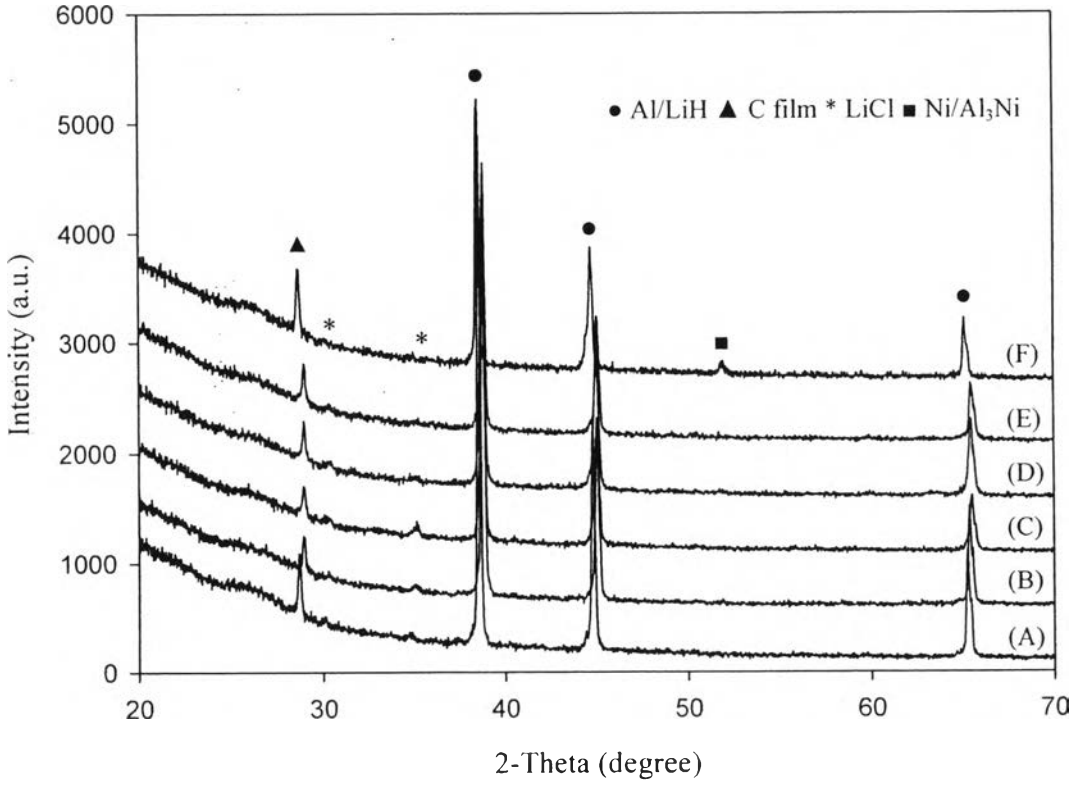

Figure 4.10 XRD patterns of dehydrogenated $LiAlH_4$ (A), dehydrogenated $LiAlH_4$ milled for 0.5 hr (B), and dehydrogenated $LiAlH_4$ mixed with 5 wt% Ti (C), 5 wt% TiO_2 (D), 5 wt% $TiCl_3$ (E), and 5 wt% Ni (F).

The dehydrogenated samples mixed with catalysts (Figure 4.10) show the same XRD patterns as that of the unmilled and milled sample after the dehydrogenation. All samples mixed with the catalysts are left with only LiCl, Al, LiH, and Ni or Al_3Ni after the dehydrogenation. There are some peaks that exist in the XRD patterns, which are not LiCl, Al, LiH. For example, in the $LiAlH_4$ and Ti systems, the dehydrogenated samples mixed with Ti compounds (Figure 4.10C-4.10E) do not show Ti peaks because they may form $Al_{1-x}Ti_{1-x}$ compound during the ball milling step. In the case of Ni, the presence 2θ of 52° may be Ni (Varin and Zbroniec, 2010) or Al_3Ni (Kojima *et al.*, 2008). The results imply that all samples mixed with the catalysts may form a new component, which acts as active species and prevents the agglomeration, which agrees with the results from Suttisawat *et al.* (2010). They found that the surface area of metal hydrides is increased by adding TiO_2. It increases the grain boundary, preserves the grain size, and prevents the agglomeration of the dehydrogenation samples.

Figure 4.11 shows XRD pattern of $LiAlH_4$ co-mixed with catalysts and CAs after the dehydrogenation. They exhibit similar results with mixing catalysts and CAs. Sample co-mixed with 5 wt% CAs and 5 wt% Ni, and Ti compounds show LiCl, LiH, Al, Al_3Ni or Ni, and Al_3Ti peaks. The XRD results indicate that both CAs and catalysts can also preserve the agglomeration of the solid metal hydrides.

4.3 Hydrogen Absorption

All dehydrogenated samples including $LiAlH_4$ mixed with CAs and catalysts, Ti, TiO_2, $TiCl_3$, and Ni, do not absorb hydrogen at 180 °C under 11 MPa hydrogen pressure. The result agrees with the previous work (Suttisawat *et al.*, 2007). Gratz *et al.* (2008) suggested that the reaction of LiH and Li_3AlH_6 to form $LiAlH_4$ in the solid state requires a thousand bars of hydrogen pressure, while the hydrogenation of LiH or Li_3AlH_6 in a THF solution requires ~1 bar hydrogen pressure at the room temperature. The temperature is one factor that affects the rehydrogenation of metal hydride. Chen *et al.* (2001) reported that the formation of

the metal hydride after the dehydrogenation still requires special conditions, high pressure, and temperature.

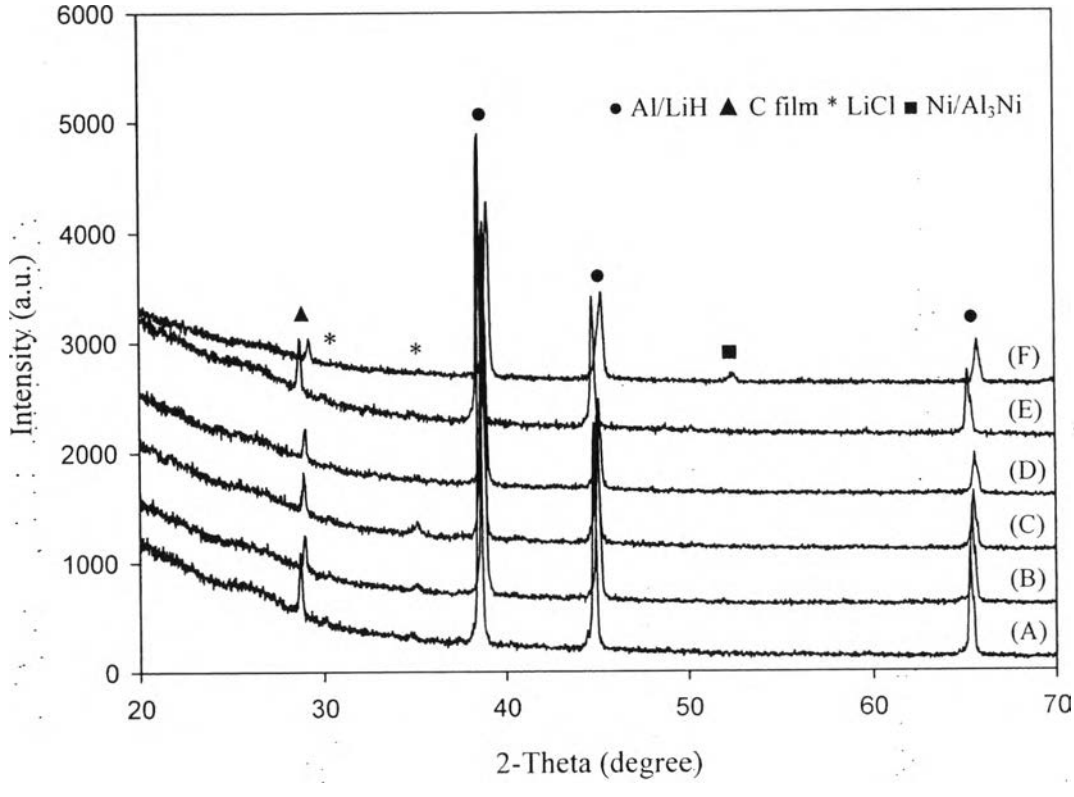

Figure 4.11 XRD patterns of dehydrogenated $LiAlH_4$ (A), dehydrogenated $LiAlH_4$ milled for 0.5 hr (B), and dehydrogenated $LiAlH_4$ co-mixed with 5 wt% CAs and 5 wt% Ti (C), 5 wt% TiO_2 (D), 5 wt% $TiCl_3$ (E), and 5 wt% Ni (F).